Environ. Sci. Technol. **2010,** *44,* 1392–1398

Effective Photocatalytic Disinfection of *E. coli* K-12 Using AgBr−Ag−Bi_2WO_6 Nanojunction System Irradiated by Visible Light: The Role of Diffusing Hydroxyl Radicals

LI-SHA ZHANG,[†] KIN-HANG WONG,[†] HO-YIN YIP,[†] CHUN HU,[‡] JIMMY C. YU,[§] CHIU-YEUNG CHAN,[∥] AND PO-KEUNG WONG*[,†,⊥]

State Key Laboratory of Environmental Aquatic Chemistry, Research Center for Eco-Environmental Sciences, Chinese Academy of Sciences, Beijing 100085, China, and Department of Biology, Department of Chemistry, Department of Microbiology, and Environmental Science Programme, The Chinese University of Hong Kong, Shatin, N.T., Hong Kong SAR, China

Received October 9, 2009. Revised manuscript received December 13, 2009. Accepted January 5, 2010.

Urgent development of effective and low-cost disinfecting technologies is needed to address the problems caused by an outbreak of harmful microorganisms. In this work, we report an effective photocatalytic disinfection of *E. coli* K-12 by using *a* AgBr−Ag−Bi_2WO_6 nanojunction system as a catalyst under visible light ($\lambda \geq 400$ nm) irradiation. The visible-light-driven (VLD) AgBr−Ag−Bi_2WO_6 nanojunction could completely inactivate 5×10^7 cfu mL^{-1} *E. coli* K-12 within 15 min, which was superior to other VLD photocatalysts such as Bi_2WO_6 superstructure, Ag−Bi_2WO_6 and AgBr−Ag−TiO_2 composite. Moreover, the photochemical mechanism of bactericidal action for the AgBr−Ag−Bi_2WO_6 nanojunction was investigated by using different scavengers. It was found that the diffusing hydroxyl radicals generated both by the oxidative pathway and the reductive pathway play an important role in the photocatalytic disinfection. Moreover, direct contact between the AgBr−Ag−Bi_2WO_6 nanojunction and bacterial cells was not necessary for the photocatalytic disinfection of *E. coli* K-12. Finally, the photocatalytic destruction of the bacterial cells was directly observed by TEM images and further confirmed by the determination of potassium ion (K^+) leakage from the killed bacteria. This work provides a potential effective VLD photocatalyst to disinfect the bacterial cells, even to destruct the biofilm that can provide shelter and substratum for microorganisms and resist to disinfection.

* Corresponding author. Tel: +852-2609 6383. Fax: 852-2603 5767. E-mail: pkwong@cuhk.edu.hk.

[†] Department of Biology, The Chinese University of Hong Kong.

[‡] Chinese Academy of Sciences.

[§] Department of Chemistry, The Chinese University of Hong Kong.

[∥] Department of Microbiology, The Chinese University of Hong Kong.

[⊥] Environmental Science Programme, The Chinese University of Hong Kong.

1. Introduction

Millions of deaths and many millions of cases of disease and disability are caused by harmful microorganisms every year (*1*). Especially, the bursting *Clostridium difficile* hospital-acquired infections, the occurrence of SARS, and the return of avian influenzas become pervasive problems afflicting people throughout the world (*2*). Disinfection by aggressive chemicals such as detergents, alcohols and chlorine components is not environmentally benign and is also ineffective for long-term (*1, 3*). Although the UV radiation is capable of sustained disinfection, the hazards of intensive and direct use of UV radiation limit its application to medical and technical purposes only (*1, 3*). Hence, alternative methods of controlling the spread and/or eradicating microorganisms are urgently needed.

Since Matsunaga et al. (*4*) reported for the first time the bactericidal effect of the TiO_2 mediated photocatalysis in 1985, the photocatalytic destruction of microorganisms has become a subject attracting much research interest (*5*). However, TiO_2 can only be activated by wavelengths in the near-UV region ($\lambda < 400$ nm), which is about 4% of the solar spectrum. Therefore, TiO_2 cannot efficiently utilize the major part of sunlight for photocatalytic disinfection. The development of efficient visible-light-driven (VLD) photocatalysts for disinfection has been a crucial issue from the viewpoint of using solar energy. Up to date, several kinds of VLD photocatalysts, such as doped or sensitized TiO_2 (*6, 7*), aurivillius oxides (*8*−*10*), and some composites (*11*), have been prepared for the degradation of organic pollutants. Only a few of them are applied to the photocatalytic disinfection of microorganisms under visible light (VL) irradiation (*12*−*16*). Furthermore, the efficiencies of VLD photocatalytic disinfection also need to be greatly improved to deal with the outbreak of harmful microorganism and to meet the high requirements of future environmental and energy problems.

Although reactive oxygen species (ROSs) including hydroxyl radical (•OH), superoxide radical ($\bullet O_2^-$) and hydrogen peroxide (H_2O_2) generated by UV-irritated TiO_2 have been revealed to be responsible for the disturbance or destruction of microorganisms (*17, 18*), the fundamental mechanism underlying the VLD photocatalytic disinfection process has not been well-established yet. For examples, little is known about the exact roles of the ROSs and whether they remain binding on the surface or diffuse into the solution bulk.

Recently, we have prepared several VLD photocatalysts including Bi_2O_3 (*19*), Bi_2WO_6 (*20*), and AgBr−Ag−Bi_2WO_6 nanojunction (*21*) for the photocatalytic degradation of organic pollutants, where AgBr−Ag−Bi_2WO_6 nanojunction is the most promising because of its double VL active components (AgBr and Bi_2WO_6) and the electron-transfer component (Ag). For a photocatalyst, it is known that there is strong correlation between the antimicrobial effect and the organic compound degradation effect (*22*). Herein, we further investigated the photocatalytic disinfection of *E. coli* K-12, a most commonly target microorganism, by using AgBr−Ag−Bi_2WO_6 nanojunction as a VLD photocatalyst. Scavengers for different kinds of ROSs were employed to investigate the roles of these species in the photocatalytic disinfection process. In particular, the partition setup reported in our previous study (*23*) had been modified in this work to confirm whether the direct contact between AgBr−Ag−Bi_2WO_6 nanojunction and the bacterial cells was a prerequisite for the photocatalytic disinfection of *E. coli* K-12.

10.1021/es903087w
Published on Web 01/19/2010

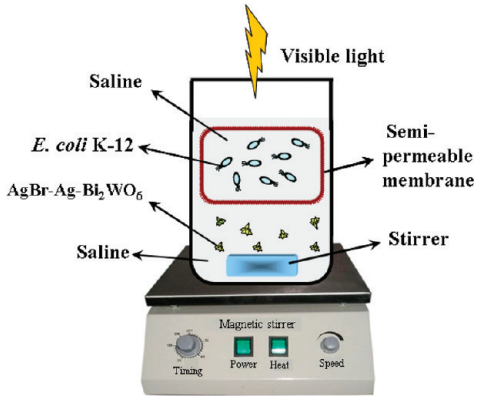

FIGURE 1. Schematic illustration of partition setup used in the photocatalytic disinfection with the AgBr−Ag−Bi_2WO_6 nanojunction as catalyst under VL irradiation.

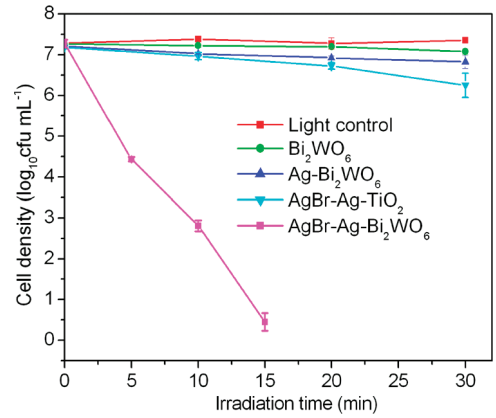

FIGURE 2. Temporal course of the *E. coli* K-12 inactivation (∼5 × 10^7 cfu mL^{-1}, 50 mL) in aqueous dispersions containing different catalysts with the same weight of each VLD component under VL irradiation. The amounts of the catalysts are 4.78 mg of Bi_2WO_6, 4.9 mg of Ag−Bi_2WO_6 containing 4.78 mg of Bi_2WO_6, 5.55 mg of AgBr−Ag−TiO_2 composite containing 0.152 mg of AgBr, and 5 mg of AgBr−Ag−Bi_2WO_6 nanojunction containing 0.152 mg of AgBr and 4.78 mg of Bi_2WO_6, respectively (*21*).

2. Experimental Section

2.1. Preparation and Characterization of Catalysts. All of the reagents were analytical grade and used without further purification. Bi_2WO_6, Ag−Bi_2WO_6, AgBr−Ag−Bi_2WO_6 nanojunction and AgBr−Ag−TiO_2 were prepared according to our previous study (*21*). Electron paramagnetic resonance (EPR) signals of paramagnetic species spin-trapped with 5,5-dimethyl-pyrroline N-oxide (DMPO) were recorded with a Bruker EPR 300E spectrometer. The irradiation source was a Quanta-Ray Nd:YAG pulsed laser system (λ=532 nm, 10 Hz).

2.2. Photocatalytic Disinfection Performance. The photocatalytic disinfection was carried out by using a 300 W xenon lamp (PLS-SXE-300, Beijing Perfect Light Co. Ltd., Beijing) as a light source (see Figure S1 in the Supporting Information). Light was passed through a UV cutoff filter ($\lambda \geq 400$ nm), and then was focused onto a flask containing a suspension of bacterial cells and photocatalyst (or the partition setup as shown in Figure 1). The visible-light intensity was measured by a light meter (LI-COR, USA) and was fixed at 190 mW cm^{-2}. All glass apparatuses used in the experiments were autoclaved at 121 °C for 20 min to ensure sterility. The bacterial cells was incubated in 10% nutrient broth solution at 30 °C for 18 h with shaking, and then washed with sterilized saline. The photocatalyst and the suspension of washed cell were then added into a flask with an aluminum cover. The final photocatalyst concentration and cell density were adjusted to 100 mg L^{-1} and about 5×10^7 or 2×10^8 colony forming units per milliliter (cfu mL^{-1}), respectively. The reaction temperature was maintained at 25 °C and the reaction mixture was stirred with a magnetic stirrer throughout the experiment. Before and after the photocatalytic oxidation (PCO) treatment, an aliquot of the reaction solution was sampled and immediately diluted with sterilized saline, and an appropriate dilution of the sample was spread on nutrient agar and incubated at 30 °C for 24 h. The number of colonies formed was counted to determine the number of viable cells.

The separated experiments were carried out using the partition setup reported recently (*23*) by replacing the Rodamine B solution inside of the semimembrane packaged container with a suspension of bacterial cells in saline as shown in Figure 1. After the desired time, 1 mL suspension inside of the container was sampled and immediately diluted. The density of living cells was then also determined by counting the cfu mL^{-1}. For comparison, the disinfection effect in this partition setup was also investigated when the outer system was replaced by Fenton reagent. All the above experiments were conducted in triplicates.

2.3. Fluorescence Spectroscopy. *E. coli* K-12 before and after PCO treatment were fluorescently stained with the dyes of LIVE/DEAD BacLight bacterial viability kit (L7012, Molecular Probes, Inc., Eugene, OR) according to procedures recommended by the manufacturer. After being incubated at 25 °C in the dark for 15 min, the samples were examined using a fluorescence microscopy (Nikon ECLIPSE 80i, Japan) equipped with a filter block N UV-2A consisting of excitation filter Ex 330−380 (Nikon, Japan) and Spot-K slider CCD camera (Diagnostic instruments. Inc., USA)

2.5. Transmission Electron Microscopy. The mixture of AgBr−Ag−Bi_2WO_6 nanojunction and *E. coli* K-12 before and after PCO treatment was sampled and centrifuged. The cells harvested were prefixed in glutaraldehyde and then trapped in low melting point agarose (LMPA). After being postfixed with osmium tetraoxide (E.M. grade, Electron Microscopy Sciences, Fort Washington, PA), the specimens trapped in LMPA were dehydrated in a graded series of ethanol and finally embedded in Spur solution (Electron Microscopy Sciences, Fort Washington, PA) for polymerization. Ultrathin sections (70 nm) were cut on an ultratome (Leica, Reichert Ultracuts, Wien, Austria) and stained with uranyl acetate and subsequently with lead citrate on copper grids. Finally, the obtained sections were examined under a JEM-1200 EXII transmission electron microscope (JEOL Ltd., Tokyo, Japan).

2.4. Quantitative Analysis of Silver and Potassium Ions. To investigate the silver ion (Ag^+) eluted from AgBr−Ag−Bi_2WO_6 nanojunction and K^+ leakage from the bacterial cells during the photocatalytic disinfection process, the AgBr−Ag−Bi_2WO_6 nanojunction/bacterial cell suspension before and after PCO treatment was respectively collected and filtered through a Millipore filter (pore size of 0.45 μm). After filtration, the solution was acidified with 3 mol L^{-1} HNO_3, and Ag^+ or K^+ concentration was measured by a polarized Zeeman atomic absorption spectrophotometer (AAS) (Hitachi Z-2300, Japan). All the above experiments were also conducted in triplicates.

3. Results and Discussion

3.1. Photocatalytic Disinfection Performance. *E. coli* K-12, a common waterborne pathogenic microorganism, was chosen as a representative microorganism to evaluate the photocatalytic disinfection performances of photocatalysts. Figure 2 shows the photocatalytic inactivation efficiencies of *E. coli* K-12 by different photocatalysts with the same weight of each VLD component under VL irradiation ($\lambda \geq 400$ nm). As a comparison, the dark control was carried out with

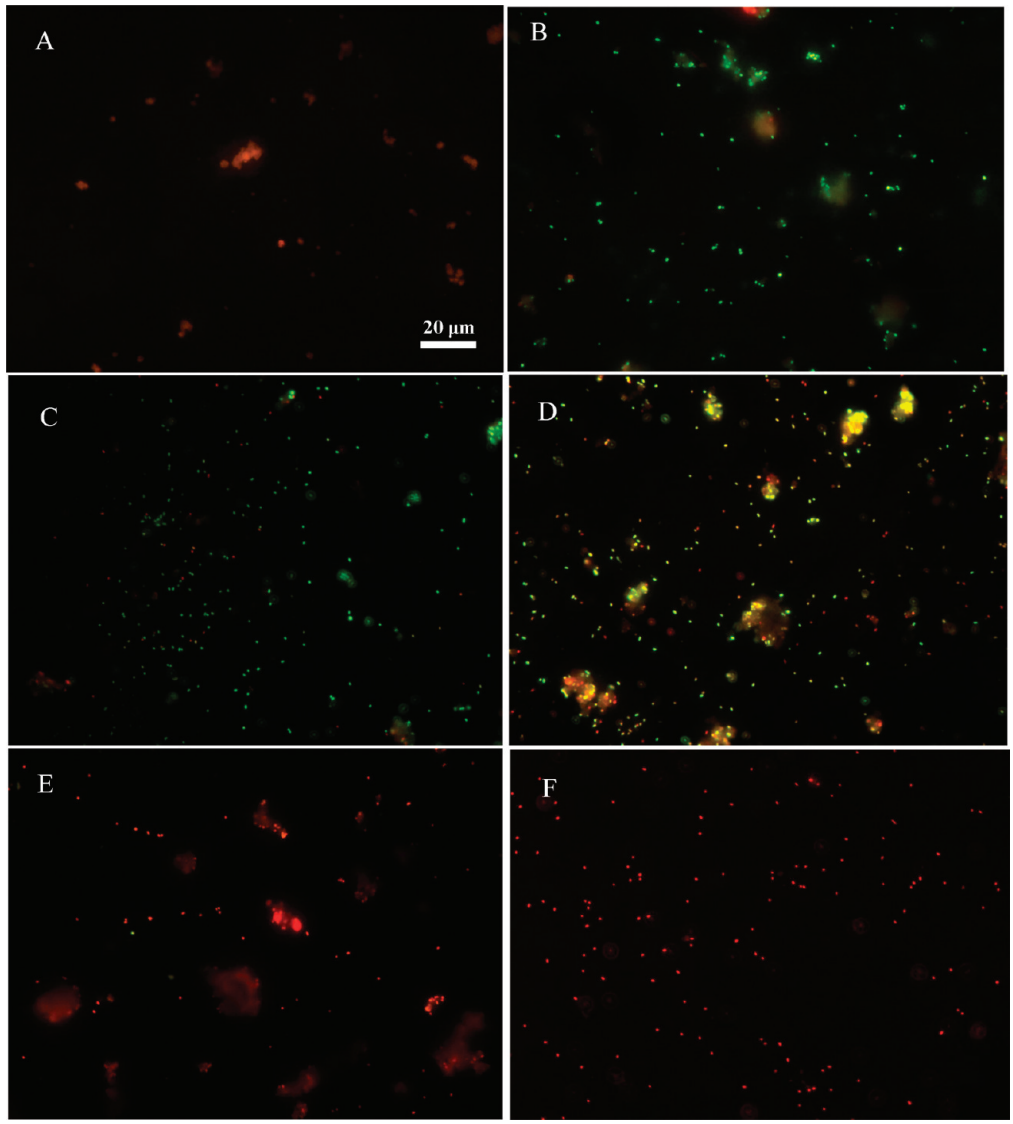

FIGURE 3. Fluorescence microscopic images of *E. coli* K-12 (~5 × 10^7 cfu mL^{-1}, 50 mL) photocatalytically untreated or treated with 5 mg of AgBr−Ag−Bi_2WO_6 nanojunction under VL irradiation. (A) Only AgBr−Ag−Bi_2WO_6 nanojunction, (B) The mixture of photocatalyst and *E. coli* K-12 before irradiation, and after irradiation by VL for (C) 1, (D) 2, (E) 5, and (F) 10 min.

different photocatalysts in dark (see Figure S2 in the Supporting Information), whereas the light control was carried out in the absence of any photocatalyst under VL irradiation (Figure 2). In the dark controls for all tested photocatalysts, the bacterial population remained constant after 30 min (see Figure S2 in the Supporting Information), indicating no toxic effect caused by the photocatalysts alone. Only visible-light irradiation also had no bactericidal effect on the bacterial cells (Figure 2). When Bi_2WO_6 was irradiated by VL, it exhibited low bactericidal activity and only 0.19 log-reduction in the vial cells count was obtained after 30 min, which is similar with the results of previous study (*14*). Although, Ag−Bi_2WO_6 and AgBr−Ag−TiO_2 samples have higher bactericidal activities under VL, only 0.4 and 1 log-inactivation were achieved within 30 min, respectively. Surprisingly, when employing AgBr−Ag−Bi_2WO_6 nanojunction as photocatalyst, 5 × 10^7 cfu mL^{-1} of *E. coli* K-12 was completely inactivated within 15 min under VL (Figure 2). Therefore, AgBr−Ag−Bi_2WO_6 nanojunction has the most excellent VLD photocatalytic inactivation performance, far exceeding those of Bi_2WO_6 superstructure, Ag−Bi_2WO_6 and AgBr−Ag−TiO_2 composite, which is consistent with its excellent photocatalytic performance on the degradation of the organic pollutant that reported in our previous study (*21*).

It is generally accepted that Ag^+ at high concentrations exhibits bactericidal activity (*24*). In our case, however, only a little amount of Ag^+, about 0.55 mg L^{-1} Ag^+, was eluted from AgBr−Ag−Bi_2WO_6 nanojunction when it was immerged in deionized water or in suspension of the bacterial cells. And there was no more Ag^+ leakage even after 5 h of photocatlaytic reaction. Moreover, no obvious bactericidal effect was observed in the presence of 0.6 mg L^{-1} Ag^+ even after 2 h (see Figure S3 in the Supporting Information). These facts suggest that the quick inactivation of *E. coli* K-12 (Figure 2) should result from the photocatalytic performance of AgBr−Ag−Bi_2WO_6 nanojunction instead of the eluted Ag^+.

To further confirm the VLD photocatalytic disinfection effect of *E. coli* K-12 using AgBr−Ag−Bi_2WO_6 nanojunction, the fluorescence assays of photocatalytically untreated and treated *E. coli* K-12 were investigated (Figure 3). These photocatalytically untreated and treated cells were stained with the mixtures of SYTO 9 green-fluorescent nucleic acid stain and the red-fluorescent nucleic acid stain, propidium iodide, which are typical cell-labeling dyes respectively for

the detection of living and dead bacteria. After stained with these dyes, AgBr−Ag−Bi_2WO_6 nanojunction could not avoid giving orange color fluorescence (Figure 3A). Notably, except the orange fluorescence emitted by catalyst, the photocatalytically untreated bacteria exhibited intense green fluorescence (Figure 3B). After being photocatalytically treated for 1 min, some bacteria exhibited red fluorescence, indicating parts of bacteria were disinfected during the VLD photocatalytic process (Figure 3C). After 2 min, the dead bacteria increased as shown in Figure 3D. Obviously, few and no living bacteria were observed respectively after 5 and 10 min (Figure 3E,F). In fact, only about 0.1% and 0.001% bacterial cells, which were calculated according to the data of Figure 2, survived after being photocatalytically treated for 5 and 10 min, respectively. On the basis of the above results, we conclude that AgBr−Ag−Bi_2WO_6 nanojunction possesses excellent VLD photocatalytic disinfection performance.

3.2. Photocatalytic Disinfection Mechanism. Our previous study has indicated that AgBr−Ag−Bi_2WO_6 nanojunction has a Z-scheme structure, where a completely separated VB-hole (Bi_2WO_6) and CB-electron (AgBr) can be generated under VL irradiation (*21*). Both the oxidation power of photogenerated VB-holes (Bi_2WO_6) (+2.68 V versus NHE) and the reduction power of photogenerated CB-electrons (AgBr) (−1.04 V versus NHE) are very strong. It is expected that the photogenerated VB-holes can oxidize the OH^- /H_2O to produce •OH (E^0 (OH^-/•OH) = 2.38 V versus NHE) (*25*), whereas the photogenerated CB-electrons can reduce the surface chemi-sorbed O_2 to produce $•O_2^-$ ($E^0(O_2/•O_2^-)$ = −0.33 V versus NHE) (*25*). To confirm this conjecture, the ESR spin-trap technique (with DMPO) was used to obtain information on the active radicals involved in irradiated or unirradiated AgBr−Ag−Bi_2WO_6 nanojunction dispersion (Figure 4). Because $•O_2^-$ in water is very unstable and undergoes facile disproportionation rather than slow reaction with DMPO (*26*), the involvement of $•O_2^-$ was examined in methanol (Figure 4A). From Figure 4A, the six characteristic peaks of the DMPO−$•O_2^-$ adducts were observed in VL irradiated AgBr−Ag−Bi_2WO_6 nanojunction dispersion. While, no $•O_2^-$ signal was detected in dark under otherwise identical conditions. Similarly, the four characteristic peaks of DMPO−•OH (1:2:2:1 quartet pattern) were also observed only in VL irradiated aqueous suspension of AgBr−Ag−Bi_2WO_6 nanojunction (Figure 4B). These facts confirm that •OH and $•O_2^-$ were produced in VL irradiated suspension of AgBr−Ag−Bi_2WO_6 nanojunction, providing a solid indication that photogenerated VB-holes (Bi_2WO_6) and CB-electrons (AgBr) could retain long enough and react with adsorbed oxygen/H_2O to produce a series of ROSs, which finally induce the decomposition of organic pollutants and/or microorganisms.

As mentioned above, ROSs generated by VL irradiated AgBr−Ag−Bi_2WO_6 nanojunction, such as •OH produced both by the oxidative pathway and the reductive pathway, $•O_2^-$ and H_2O_2, are potentially involved in the disinfection process of *E. coli* K-12 (*17, 18*). To find out the exact kind(s) of these ROSs playing significant role(s) in the disinfection process, as shown in Figure 5, we further investigated the photocatalytic disinfection of *E. coli* K-12 by respectively suppressing the •OH-mediated process with alcohol scavenger (*27, 28*), testifying oxidative pathway with sodium oxalate as hole scavenger (*29*), eliminating the effect of ROSs generated at the reduction site with Cr(VI) as an electron scavenger (*27*), and enhancing the generation of the bulk phase free •OH by reacting photocatalytically generated H_2O_2 with Fe(II) (*18*). The control experiments show that the addition of each of these scavengers with as mentioned concentration had no toxic effect on *E. coli* K-12 within 15 min (see Figure S4 in the Supporting Information). Without any scavenger, the density of *E. coli* K-12 sharply declined to 2 cfu mL^{-1} after 15-min photocatalytic treatment (Figure 5). In the presence

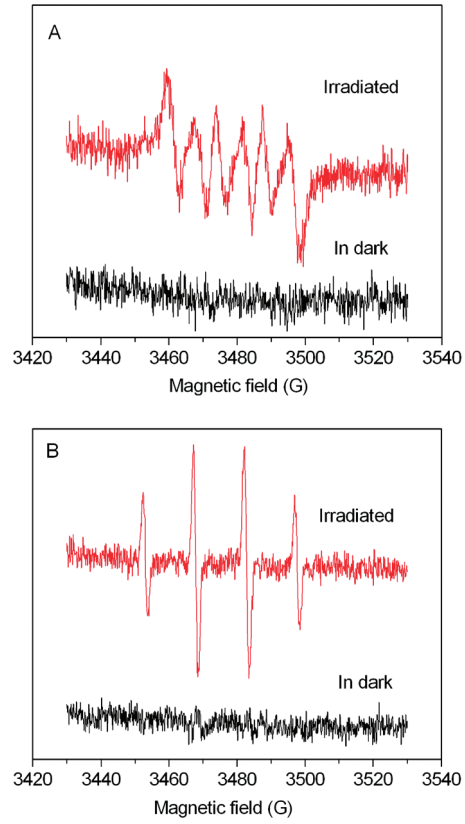

FIGURE 4. DMPO spin-trapping ESR spectra recorded at ambient temperature in AgBr−Ag−Bi_2WO_6 nanojunction suspension under VL irradiation (λ=532 nm). (A) For DMPO−$•O_2^-$ in methanol dispersion, and (B) For DMPO−•OH in aqueous dispersion.

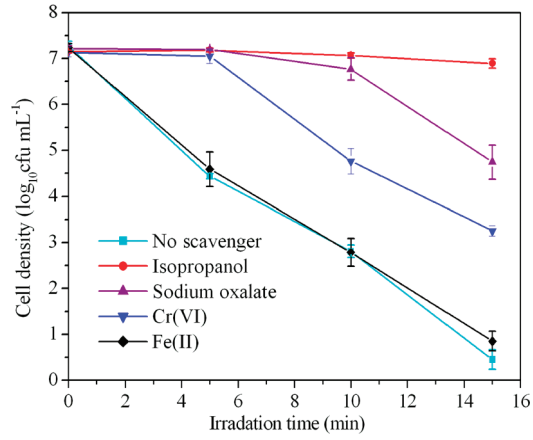

FIGURE 5. Photocatalytic disinfection of *E. coli* K-12 by AgBr−Ag−Bi_2WO_6 nanojunction respectively with different scavengers (0.05 mmol L^{-1} Cr(VI), 2 μmol L^{-1} Fe(II)-EDTA, 0.3 mol L^{-1} isopropanol, 30 μmol L^{-1} sodium oxalate) under VL irradiation.

of sodium oxalate (a hole scavenger), the density of *E. coli* K-12 only declined to 6×10^4 cfu mL^{-1} after 15 min irradiation, indicating the involvement of •OH generated by the oxidative pathway in the photocatalytic disinfection. With the addition of Cr(VI) (a electron scavenger), the density of *E. coli* K-12 also only dropped to 2×10^3 cfu mL^{-1} after 15 min, which results from the fact that the electron can reduce the absorbed oxygen to generate $•O_2^-$. Although the produced $•O_2^-$ in water is very unstable, it would subsequently undergo facile disproportionation to produce other ROSs including H_2O_2 and •OH (*26*). In addition, the introduction of Fe^{2+} can usually

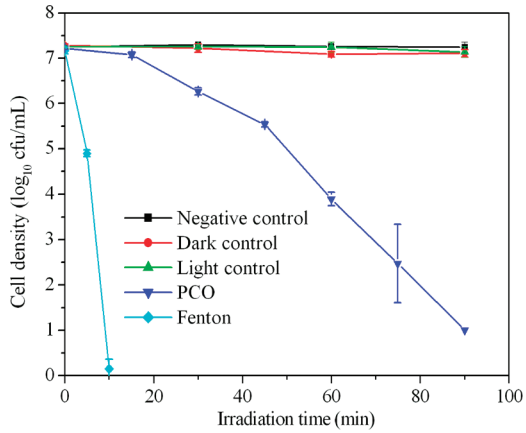

FIGURE 6. Photocatalytic disinfection of *E. coli* K-12 (~5 × 10^7 cfu mL^{-1}, 20 mL) inside a semipermeable membrane packaged container when the outer system is in various conditions (PCO: Saline + 5 mg AgBr−Ag−Bi_2WO_6 nanojunction + VL irradiation; Fenton: Saline + Fenton reagent (4 mmol L^{-1} H_2O_2 + 10 mmol L^{-1} Fe(II)-EDTA) (*30*).

improve the generation of the bulk phase free •OH by reacting with H_2O_2 (Fenton reaction) and therefore enhance the inactivation path by the resulting free •OH (*18*). In this case, however, no obvious enhancement of photocatalytic disinfection efficiency was obtained by the addition of Fe^{2+}, indicating that there was little H_2O_2 involved. Therefore, during this AgBr−Ag−Bi_2WO_6 nanojunction mediated VLD photocatalytic process, •OH generated by both of the oxidative pathway and reductive pathway was mainly responsible for the disinfection of *E. coli* K-12.

To clarify whether the disinfection of *E. coli* K-12 was caused by •OH remaining bound to the surface or those diffusing into the solution bulk, isopropanol was employed as a diagnostic tool for the diffusing •OH because it is easily oxidized by •OH and has low affinity to semiconductor surfaces in aqueous media (*27, 28*). Interestingly, as can be seen from Figure 5, the addition of isopropanol could almost completely inhibit the photocatalytic disinfection of *E. coli* K-12, which indicates that the free •OH in the aqueous suspension plays an important role. Our previous study has proved that AgBr−Ag−Bi_2WO_6 nanojunction in neutral solution possess negative charge (*21*), which is the same with surface charge of *E. coli* K-12 (*13*). Thus, the electrostatic repulsion and the motility of bacteria result in that •OH remaining bound to the surface has little chance to disinfect the major portion of bacterial cells. As expected, the equilibrium adsorption time of *E. coli* K-12 over AgBr−Ag−Bi_2WO_6 nanojunction before photocatalytic process had no significant effect on the photocatalytic disinfection (see Figure S5 in the Supporting Information).

To further confirm the role of the diffusing •OH, we also conducted the photocatalytic disinfection of *E. coli* K-12 using the partition setup (Figure 1). As shown in Figure 1, a suspension of *E. coli* K-12 in saline was contained in the membrane packaged container and the photocatalyst particles dispersed in the saline outside of the container. Here, the semipermeable membrane with the molecular weight cutoff (MWCO) of 12 000−14 000 Da allowed the free entry of smaller molecules such as water and diffusing •OH, but prevented the passage of larger targets such as the AgBr−Ag−Bi_2WO_6 nanojunction with the diameter sizes of about 3 μm (*21*) and *E. coli* K-12 with molecular weight of about 2.6 × 10^6 daltons. Figure 6 shows the disinfection efficiency of *E. coli* K-12 inside a membrane packaged container when the outer system was under various conditions. As shown in Figure 6, there were no obvious inactivation of *E. coli* K-12 in the control experiments, revealing that the catalyst or light itself have no toxic effect on *E. coli* K-12 even after 1.5 h. To our surprise, there was about 6.5 log-reduction in viable cells count within 1.5 h when the outer system was VL irradiated AgBr−Ag−Bi_2WO_6 nanojunction suspension. Since the VL irradiated AgBr−Ag−Bi_2WO_6 nanojunction and *E. coli* K-12 were separated by the semipermeable membrane, only the diffusing reactive oxygen radicals, such as the diffusing •OH generated by VLD AgBr−Ag−Bi_2WO_6 nanojunction, could pass through the semipermeable membrane to inactivate the bacterial cells inside of container. When the outer system was replaced by a Fenton reagent, a typical homogeneous system to generate bulky •OH, almost all of *E. coli* K-12 were disinfected within 10 min, which further confirms that the diffusing •OH could go through the

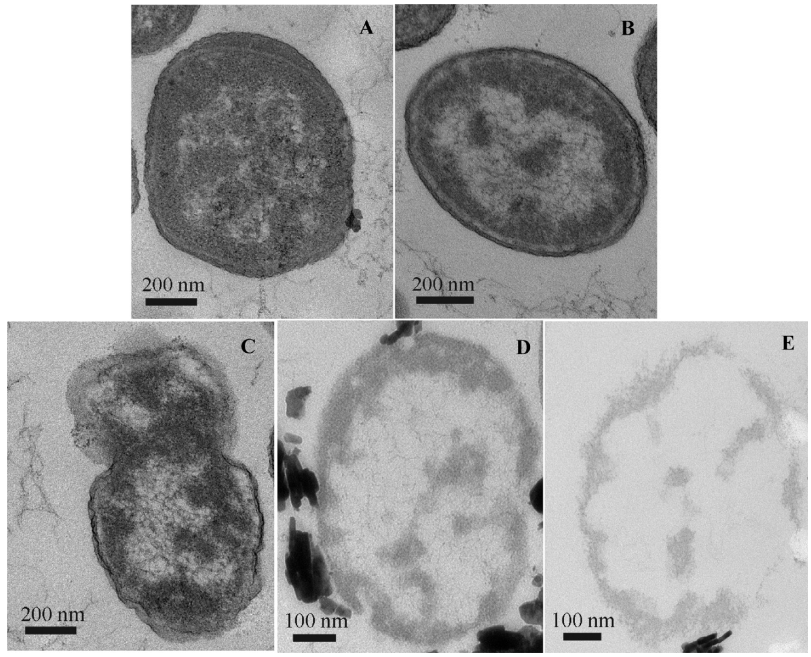

FIGURE 7. TEM images of *E. coli* K-12 photocatalytically untreated or treated with AgBr−Ag−Bi_2WO_6 nanojunction under VL irradiation. (A) Before irradiation, and after irradiated for (B) 15 min, (C) 30 min, (D) 4 h, and (E) 8 h.

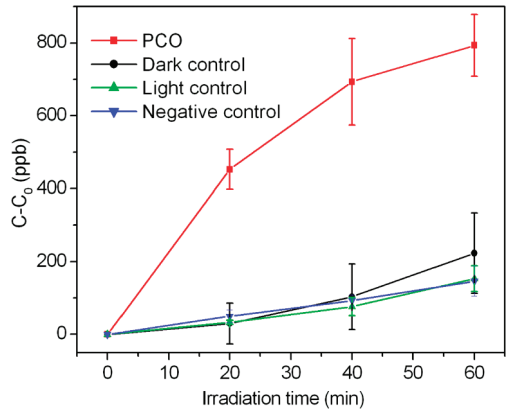

FIGURE 8. Potassium ion (K^+) leakage from *E. coli* K-12 under different conditions (PCO: AgBr−Ag−Bi_2WO_6 nanojunction with visible light irradiation; dark control: only AgBr−Ag−Bi_2WO_6 nanojunction; light control: only visible light irradiation; negative control: no light and no catalyst).

membrane to inactivate the bacterial cells inside the container. Although the disinfection efficiency of *E. coli* K-12 by the Fenton reagent was higher than that by the VLD AgBr−Ag−Bi_2WO_6 nanojunction, the Fenton reagent would quickly lose its effect after the complete consumption of H_2O_2 (*30*), while VLD AgBr−Ag−Bi_2WO_6 nanojunction is predicted to persist for long time due to its high stability confirmed by our previous study (*21*). The photocatalytic disinfection efficiency of *E. coli* K-12 in the partition system (Figure 6) was lower than that in the nonseparated system (Figure 2) because the lifetime of •OH is short and some of them may annihilate during the diffusing process (*31*). But of importance is that this fact directly proves that the direct contact between AgBr−Ag−Bi_2WO_6 nanojunction and bacterial cells is not a prerequisite for photocatalytic disinfection of microorganism.

To understand the destruction process of bacteria by the diffusing •OH generated by VLD AgBr−Ag−Bi_2WO_6 nanojunction, the structure and morphology of *E. coli* K-12 at the different stages of PCO was examined by TEM studies (Figure 7). Before the PCO process, *E. coli* K-12 exhibited a well-defined cell wall as well as the evenly rendered interior of the cell (Figure 7A), which corresponds to the presence of proteins and DNA. Only after 15-min photocatalytic treatment, an electron translucent region and the filament-like structure appeared at the central of the cell (Figure 7B), which indicates that the outer membrane of the cell was damaged and therefore a leakage of the interior component occurred. This observation is well matched with the previous study that significant disorder in membrane permeability can be caused by the attack of photogenerated •OH (*32*). Potassium ion (K^+), a component virtually existing in bacteria and involving in the regulation of polysome content and protein synthesis, quickly leaked from the bacteria during the PCO process (Figure 8) because of the permeability change of membrane, resulting in the loss of cell viability (*14, 33*). In contrast, there is no significant leakage of K^+ occurred in the three sets of control experiments (dark control, light control, and negative control) (Figure 8). These facts also confirm that the disinfection of *E. coli* K-12 resulted from the generated •OH during photocatalytic process instead of the Ag^+ eluted from catalyst and/or the Ag nanoshell in AgBr−Ag−Bi_2WO_6 nanojunction. After 30 min of irradiation, great changes had taken place to the morphology of *E. coli* K-12 (Figure 7C). The cell structure was severely distorted and the cell wall was greatly ruptured, which facilitated the entry of large amount of diffusing •OH to further degrade the left intracellular components of the cells. Due to its powerful oxidative ability, •OH could effectively degrade these remaining cell components. Therefore, with the prolonged irradiation time, the whole cell became more translucent (Figure 7D). Eventually, there was only a small portion of cell debris (Figure 7E), which demonstrated a complete destruction of bacterial cell.

Therefore, it is concluded that the AgBr−Ag−Bi_2WO_6 nanojunction has great potential for photocatalytic destruction of microorganisms. It should work well in biofilms that are resilient to disinfection because biofilms can provide shelter and substratum for microorganisms, store and trap nutrient, and support microbial multiplication extracellularly. This future development is being investigated by our group.

Acknowledgments

The project was supported by a research grant (CUHK4585/06M) from the Research Grant Council, Hong Kong SAR Government, to P.K.W., C.H., J.C.Y., and C.Y.C. The authors also thank Mr. Freddie Kwok of The Chinese University of Hong Kong for assistance in the TEM observation.

Supporting Information Available

Additional details in five figures (PDF). This material is available free of charge via the Internet at http://pubs.acs.org.

Literature Cited

(1) Shannon, M. A.; Bohn, P. W.; Elimelech, M.; Georgiadis, J. G.; Mariñas, B. J.; Mayes, A. M. Science and technology for water purification in the coming decades. *Nature* **2008**, *452*, 301–310.
(2) Chung, C. J.; Lin, H. I.; Tsou, H. K.; Shi, Z. Y.; He, J. L. An antimicrobial TiO_2 coating for reducing hospital-acquired infection. *J. Biomed. Mater. Res., B* **2008**, *85B*, 220–224.
(3) Erkan, A.; Bakir, U.; Karakas, G. Photocatalytic microbial inactivation over Pd-doped SnO_2 and TiO_2 thin films. *J. Photochem. Photobiol., A* **2006**, *184*, 313–321.
(4) Matsunaga, T.; Tomada, R.; Nakajima, T.; Wake, H. Photoelectrochemical sterilization of microbial cells by semiconductor powders. *FEMS Microbiol. Lett.* **1985**, *29*, 211–214.
(5) Blake, D. M.; Maness, P. C.; Huang, Z.; Wolfrum, E. J.; Huang, J.; Jacoby, W. A. Application of the photocatalytic chemistry of titanium dioxide to disinfection and the killing of cancer cells. *Sep. Purif. Meth.* **1999**, *28*, 1–50.
(6) Asahi, R.; Morikawa, T.; Ohwaki, T.; Aoki, K.; Taga, Y. Visible-light photocatalysis in nitrogen-doped titanium oxides. *Science* **2001**, *293*, 269–271.
(7) Zhang, M.; Chen, C. C.; Ma, W. H.; Zhao, J. C. Visible-light-induced aerobic oxidation of alcohols in a coupled photocatalytic system of dye-sensitized TiO_2 and TEMPO. *Angew. Chem., Int. Ed.* **2008**, *47*, 9730–9733.
(8) Tang, J.; Zou, Z. G.; Ye, J. H. Efficient photocatalytic decomposition of organic contaminants over $CaBi_2O_4$ under visible-light irradiation. *Angew. Chem., Int. Ed.* **2004**, *43*, 4463–4466.
(9) Zhang, C.; Zhu, Y. Synthesis of square Bi_2WO_6 nanoplates as high-activity visible-light-driven photocatalysts. *Chem. Mater.* **2005**, *17*, 3537–3545.
(10) Zhang, L. Z.; Djerdj, I.; Cao, M. H.; Antonietti, M.; Niederberger, M. Nonaqueous sol-gel synthesis of a nanocrystalline $InNbO_4$ visible-light photocatalyst. *Adv. Mater.* **2007**, *19*, 2083–2086.
(11) Liu, Z. F.; Zhao, Z. G.; Miyauchi, M. Efficient visible light active $CaFe_2O_4/WO_3$ based composite photocatalysts: Effect of interfacial modification. *J. Phys. Chem. C* **2009**, *113*, 17132–17137.
(12) Yu, J. C.; Gkeiho, W.; Yu, J. G.; Yip, H. Y.; Wong, P. K.; Zhao, J. C. Efficient visible-light-induced photocatalytic disinfection on sulfur-doped nanocrystalline titania. *Environ. Sci. Technol.* **2005**, *39*, 1175–1179.
(13) Hu, C.; Hu, X. X.; Guo, J.; Qu, J. H. Efficient destruction of pathogenic bacteria with $NiO/SrBi_2O_4$ under visible light irradiation. *Environ. Sci. Technol.* **2006**, *40*, 5508–5513.
(14) Ren, C.; Wang, W. Z.; Zhang, L.; Chang, J.; Sheng, H. Photocatalytic inactivation of bacteria by photocatalyst Bi_2WO_6 under visible light. *Catal. Commun.* **2009**, *10*, 1940–1943.
(15) Li, Q.; Li, Y. W.; Wu, P. G.; Xie, R. C.; Shang, J. K. Palladium oxide nanoparticles on nitrogen-doped titanium oxide: accelerated photocatalytic disinfection and post-illumination catalytic memory". *Adv. Mater.* **2008**, *20*, 3717–3723.
(16) Ren, C.; Wang, W. Z.; Sun, S. M.; Zhang, L.; Chang, J. Enhanced photocatalytic activity of Bi_2WO_6 loaded with Ag nanoparticles

under visible light irradiation. *Appl. Catal., B* **2009**, *92*, 50–55.
(17) Maness, P. C.; Smolinski, S.; Blake, D. M.; Huang, Z.; Wolfrum, E. J.; Jacoby, W. A. Bactericidal activity of photocatalytic TiO_2 reaction: Toward an understanding of its killing mechanism. *Appl. Environ. Microbiol.* **1999**, *65*, 4094–4098.
(18) Cho, M.; Chung, H.; Choi, W. Y.; Yoon, J. Y. Different inactivation behaviors of MS-2 phage and *Escherichia coli* in TiO_2 photocatalytic disinfection. *Appl. Environ. Microbiol.* **2005**, *71*, 270–275.
(19) Zhang, L. S.; Wang, W. Z.; Yang, J.; Chen, Z. G.; Zhang, W. Q.; Zhou, L.; Liu, S. W. Sonochemical synthesis of nanocrystallite Bi_2O_3 as a visible-light-driven photocatalyst. *Appl. Catal. A* **2006**, *308*, 105–110.
(20) Zhang, L. S.; Wang, W. Z.; Chen, Z. G.; Zhou, L.; Xu, H. L.; Zhu, W. Fabrication of flower-like Bi_2WO_6 superstructures as high-performance visible-light driven photocatalysts. *J. Mater. Chem.* **2007**, *17*, 2526–2532.
(21) Zhang, L. S.; Wong, K. H.; Chen, Z. G.; Yu, J. C.; Zhao, J. C.; Hu, C.; Chan, C. Y.; Wong, P. K. AgBr-Ag-Bi_2WO_6 nanojunction system: A novel and efficient photocatalyst with double visible-light active components. *Appl. Catal., A* **2009**, *363*, 221–229.
(22) Chen, F. N.; Yang, X. D.; Wu, Q. Photocatalytic oxidation of *Escherischia coli*, *Aspergillus niger*, and formaldehyde under different ultraviolet irradiation conditions. *Environ. Sci. Technol.* **2009**, *43*, 4606–4611.
(23) Zhang, L. S.; Wong, K. H.; Zhang, D. Q.; Hu, C.; Yu, J. C.; Chan, C. Y.; Wong, P. K. Zn:$In(OH)_yS_z$ solid solution nanoplates: synthesis, characterization, and photocatalytic mechanism. *Environ. Sci. Technol.* **2009**, *43*, 7883–7888.
(24) Pal, S.; Tak, Y. K.; Song, J. M. Does the antibacterial activity of silver nanoparticles depend on the shape of the nanoparticle? A study of the Gram-negative bacterium *Escherichia coli*. *Appl. Environ. Microbiol.* **2007**, *73*, 1712–1720.
(25) Li, Z. H.; Dong, T. T.; Zhang, Y. F.; Wu, L.; Wang, J. Q.; Wang, X. X.; Fu, X. Z. Studies on $In(OH)_yS_z$ solid solutions: Syntheses, characterizations, electronic structure, and visible-light-driven photocatalytic activities. *J. Phys. Chem. C* **2007**, *111*, 4727–4733.
(26) Ma, W.; Huang, Y.; Li, J.; Chen, M.; Song, W.; Zhao, J. An efficient approach for the photodegradation of organic pollutants by immobilized iron ions at neutral pHs. *Chem. Commun.* **2003**, 1582–1583.
(27) Chen, Y. X.; Yang, S. Y.; Wang, K.; Lou, L. P. Role of primary active species and TiO_2 surface characteristic in UV-illuminated photodegradation of Acid Orange 7. *J. Photochem. Photobiol., A.* **2005**, *172*, 47–54.
(28) Khodja, A. A.; Boulkamh, A.; Richard, C. Phototransformation of metobromuron in the presence of TiO_2. *Appl. Catal. B* **2005**, *59*, 147–154.
(29) Jin, R. C.; Gao, W. L.; Chen, J. X.; Zeng, H. S.; Zhang, F. X.; Liu, Z. G.; Guan, N. J. Photocatalytic reduction of nitrate ion in drinking water by using metal-loaded $MgTiO_3-TiO_2$ composite semiconductor catalyst. *J. Photochem. Photobiol., A* **2004**, *162*, 585–590.
(30) Zhang, L. S.; Li, J. L.; Chen, Z. G.; Tang, Y. W.; Yu, Y. Preparation of Fenton reagent with H_2O_2 generated by solar light-illuminated nano-Cu_2O/MWNTs composites. *Appl. Catal., A* **2006**, *299*, 292–297.
(31) Ishikawa, Y.; Matsumoto, Y.; Nishida, Y.; Taniguchi, S.; Watanabe, J. Surface treatment of silicon carbide using TiO_2(IV) photocatalyst. *J. Am. Chem. Soc.* **2003**, *125*, 6558–6562.
(32) Cheng, Y. W.; Chan, C. Y.; Wong, P. K. Disinfection of *Legionella pneumophila* by photocatalytic oxidation. *Water Res.* **2007**, *41*, 842–852.
(33) Saito, T.; Iwase, T.; Horie, J.; Morioka, T. Mode of photocatalytic bactericidal action of powdered semiconductor TiO_2 on mutans streptococci. *J. Photochem. Photobiol., B* **1992**, *14*, 369–379.

ES903087W